Inorganic Chemistry

Article

pubs.acs.org/IC

Synthesis of a "Super Bulky" Guanidinate Possessing an Expandable Coordination Pocket

Arnab K. Maity, Skye Fortier,* Leonel Griego, and Alejandro J. Metta-Magaña

Department of Chemistry, University of Texas at El Paso, El Paso, Texas 79968, United States

Supporting Information

ABSTRACT: Friedel–Crafts alkylation of 4-*tert*-butylaniline with 2 equiv of benzhydrol affords bulky 2,6-bis-(diphenylmethyl)-4-*tert*-butylaniline (**Ar*NH$_2$**) in good yield, which can be readily synthesized on a tens of grams scale. The reaction of 6 equiv of **Ar*NH$_2$** with triphosgene generates the symmetric urea **(Ar*NH)$_2$CO**, which, upon dehydration with a P_2O_5/Al_2O_3 slurry in pyridine, produces the sterically encumbered carbodiimide **(Ar*N)$_2$C** as an air-stable white solid. The treatment of **(Ar*N)$_2$C** with LiN=C^{t}Bu$_2$ in tetrahydrofuran cleanly gives the monomeric lithium guanidinate **Li[^{Ar}*ketguan]**, free of coordinating solvent, in 85% yield. Protonation of **Li[^{Ar}*ketguan]** with lutidinium chloride produces the guanidine **^{Ar}*ketguanH** (MW = 1112.60 g/mol), which is easily derivatized to give the monomeric alkali metal complexes **M[^{Ar}*ketguan]** (M = K, Cs) in 94% and 51% yield, respectively. The solid-state molecular structures of **M[^{Ar}*ketguan]** (M = Li, K, Cs) show formally two-coordinate alkali metal cations encapsulated within a hydrophobic coordination pocket formed by the peripheral diphenylmethyl substituents of the guanidinate. Remarkably, percent buried volume analyses (% V_{Bur}) of **M[^{Ar}*ketguan]** [M = Li (94.8% V_{Bur}), K (92.1% V_{Bur}), Cs (81.7% V_{Bur})] reveal a coordination cavity that adjusts to individually accommodate the variously sized metal ions despite the highly encumbering nature of the ligand. This demonstrates a flexible ligand framework that is able to stabilize low-coordinate metal centers within a "super bulky" coordination environment.

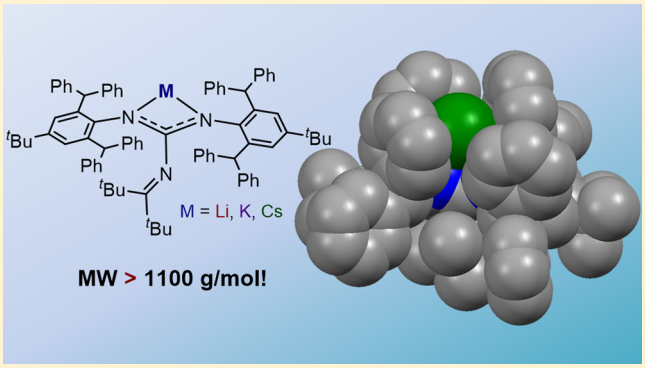

INTRODUCTION

The kinetic stabilization provided by sterically encumbering ligands has enabled the synthesis of a wide range of metal complexes featuring rare and remarkable bonding motifs with unique reactivity patterns—motifs, in many cases, that would otherwise be deemed too reactive or unstable for isolation. For instance, triamidoamines, $[\{RN(CH_2)_n\}_3N]^{3-}$, are a popular class of bulky tetradentate ligands that have been used with metals for the capture and activation of small molecules. Upon coordination, triamidoamines encapsulate a metal wherein the pendant R groups form a hydrophobic cavity or "pocket" through which the metal can be accessed. This feature has allowed the trapping of weakly coordinating N_2O with vanadium in $[\{RN(CH_2)_n\}_3N]V(N_2O)$ (R = 5-mesitylpyrrole; n = 1),[1] has been used in the activation of O_2 and stabilization of the first structurally characterized terminal iron(III) oxo in $[\{RN(CH_2)_n\}_3N]Fe(O)$ (R = (*N*′-*tert*-butylureaylato; n = 2),[2] and has been employed in the capture of N_2 with $[\{RN(CH_2)_n\}_3N]Mo$ (R = hexaisopropylterphenyl; n = 2) for its catalytic reduction to NH_3,[3] and to prevent nitride bridging and cluster aggregation in $[\{RN(CH_2)_n\}_3N]U(N)$ (R = triisopropylsilyl; n = 2) to give the first terminal uranium nitride.[4] Likewise, other encapsulating or cavity-forming ligands have been used to similar ends including the κ^6-alkoxytriazacyclononane-supported uranium(III) complex $[(^{Ad}ArO)_3tacn]U$ [$(^{Ad}ArO)_3tacn$ = tris(3-adamantyl-5-*tert*-butyl-2-hydroxybenzyl)triazacyclononane], which binds and reduces CO_2 to give the uranium(IV) species $[(^{Ad}ArO)_3tacn]U(\eta^1\text{-}O{=}C^{\bullet}\text{-}O^{-})$,[5] while the scorpionate-type triscarbene [PhB-(^{t}BuIm)$_3$]$^-$ [PhB(^{t}BuIm)$_3$ = phenyltris(3-*tert*-butylimidazol-2-ylidene)borato] has facilitated isolation of the cationic iron(V) nitride $[\{PhB(^tBuIm)_3\}FeN][BAr^f]$,[6] just to name a few examples.

Furthermore, highly encumbering ligands with low-coordination modes can force metals to adopt unsaturated geometries. This phenomenon can give rise to metal complexes that exhibit unusual electronic structures or rare bonding modes.[7] For example, the chromium(I) aryl complex Ar′CrCrAr′ [Ar′ = 2,6-(2′,6′-diisopropylphenyl)terphenyl] features a Cr–Cr quintuple bond, with each Cr displaying a severely bent two-coordinate geometry.[7a] Bulky guanidinates and β-diketiminates have been utilized to synthesize three-coordinate, monovalent metal compounds with unprecedented, unsupported metal–metal bonds such as those in the magnesium(I) complex $[\{(^{dipp}ArN)_2C(R)\}Mg]_2$ (^{dipp}Ar = 2,6-

Received: May 24, 2014
Published: July 16, 2014

   dx.doi.org/10.1021/ic501219q | *Inorg. Chem.* 2014, 53, 8155–8164

diisopropylphenyl; R = diisopropylamide) and the manganese(I) complex $[\{HC(CMeN^{dipp}Ar)_2\}Mn]_2$.[7c,e,8] Additionally, bulky aryls,[7f,k] alkoxides,[7i,9] and amides[7b,f] have been used to generate two-coordinate, open-shell transition-metal complexes, including the linearly coordinated vanadium(II) complex $[^{iPr6}Ar(H)N]_2V$ [^{iPr6}Ar = 2,6-(2′-4′-6′-triisopropylphenyl)terphenyl],[7b] and have even enabled the synthesis of a wide range of compounds possessing multiply bonded main-group elements.[7d] Finally, to provide fine kinetic control, massive coligands have also found use in catalysis.[10]

Clearly, sterically encumbering ligands constitute an important ligand class given the pronounced effect that they can have on the structure and reactivity of metals. Thus, the design and synthesis of new and novel sterically demanding ligands is needed to continue to explore new routes to achieving unique and challenging chemical transformations. To this end, our laboratory has been targeting the synthesis of highly encumbering, or "super bulky", ligands based on the popular guanidine scaffold, in particular, those that combine the properties and characteristics of *both* encapsulating and low-coordinating ligand classes.

We herein report the facile synthesis and characterization of the new guanidinate $[(Ar^*N)_2C(R)]^-$ [$[^{Ar}$***ketguan**$]^-$; Ar* = 2,6-bis(diphenylmethyl)-4-*tert*-butylphenyl and R = $NC(^tBu)_2$], which can be easily synthesized in a few steps on a multigram scale. Compared to other "bulky" guanidinate platforms[11] (or their formamidinate or amidinate counterparts), $[^{Ar}$***ketguan**$]^-$ is unparalleled in scope and size and thus is best categorized as belonging to a "super bulky" class unto its own. Moreover, $[^{Ar}$***ketguan**$]^-$ features a cylindrical hydrophobic binding pocket, a characteristic not typical of guanidinates but similar to those found in triamidoamines, while simultaneously maintaining a low κ^2-coordination mode. Quite notably, examination of its coordination profile with a range of group 1 cations, as determined by structural analyses and percent buried volume calculations, reveals the coordination pocket of $[^{Ar}$***ketguan**$]^-$ to be highly encumbering yet geometrically flexible, or expandable, and able to accommodate metal ions of disparate sizes.

RESULTS AND DISCUSSION

Syntheses. We chose to use a guanidine framework for the assembly of our "super bulky" ligand because guanidines are highly modular and robust ligands with generally straightforward syntheses.[12] Additionally, guanidines most commonly coordinate via a tweezer-like κ^2-ligation mode, which, with sufficiently encumbering pendant groups, could foreseeably act to encapsulate a metal in a hinged clamshell fashion. The first step toward accomplishing this required the synthesis of the encumbering, but sterically flexible,[13] aniline **Ar*NH$_2$** [Ar* = 2,6-bis(diphenylmethyl)-4-*tert*-butylphenyl]. Following the protocol of Markó et al.,[10b,13] **Ar*NH$_2$** was synthesized in 80% yield from the solvent-free Friedel–Crafts alkylation of 4-*tert*-butylaniline with benzhydrol (eq 1), a reaction that we performed up to a 60 g scale.

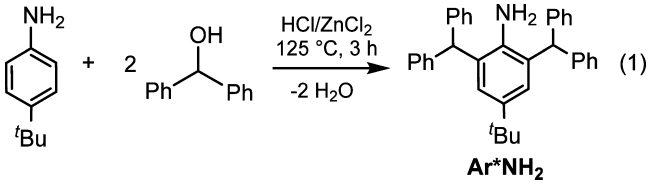

Ar*NH$_2$ is highly soluble in polar solvents such as $CHCl_3$ and tetrahydrofuran (THF) but sparingly soluble in alcohols or aliphatics such as methanol (MeOH) or hexane. The ^{1}H NMR spectrum of **Ar*NH$_2$** in $CDCl_3$ reveals three singlets at 0.98, 3.28, and 5.47 ppm corresponding to the *tert*-butyl, amine, and methine protons, respectively. The *ortho*, *para*, and *meta* protons of the phenyl substituents appear as three well-separated multiplets at 7.10, 7.22, and 7.29 ppm, respectively, while the *m*-*N*-aryl protons of the aniline ring appear slightly upfield as a singlet at 6.58 ppm.

Dehydrothiolation of thioureas or dehydration of ureas generates carbodiimides, which serve as versatile guanidine precursors.[12] Our attempts to synthesize a thiourea from **Ar*NH$_2$** were unsuccessful; however, the addition of triphosgene to a CH_2Cl_2 solution containing 6 equiv of **Ar*NH$_2$**, in the presence of 6 equiv of *p*-(dimethylamino)-pyridine (DMAP), followed by heating under reflux conditions for 15 days, cleanly afforded the bulky urea **(Ar*NH)$_2$CO** in 86% yield (eq 2).[14] **(Ar*NH)$_2$CO** is insoluble in aliphatic

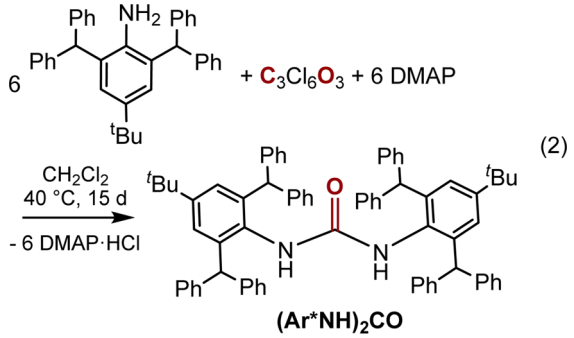

solvents, partially soluble in arenes such as toluene, and fully soluble in THF and $CHCl_3$. The ^{1}H NMR spectrum of **(Ar*NH)$_2$CO** in C_6D_6 exhibits diagnostic *tert*-butyl, amine, and methine resonances at 1.05, 4.55, and 6.31 ppm in an expected 18:2:4 ratio, respectively, consistent with a 2-fold geometry in solution. Notably, the aryl protons from the diastereotopic diphenylmethyl substituents appear in the ^{1}H NMR spectrum as a single set of multiplets at 6.99, 7.07, and 7.38 ppm in a 8:16:16 ratio, respectively, while the $^{13}C\{^1H\}$ NMR spectrum shows only eight resonances attributable to the carbon atoms of both the aniline and phenyl rings. Altogether, these observations suggest that rotation of the pendant NAr* moieties about the N–C_{ipso} bonds in **(Ar*NH)$_2$CO** is not hindered and is sufficiently rapid, on the NMR time scale, to exchange the positions of the diastereotopic phenyl rings of the diphenylmethyl groups. Finally, the $^{13}C\{^1H\}$ NMR spectrum also shows a distinctive carbonyl resonance at 154.7 ppm, while the IR spectrum of **(Ar*NH)$_2$CO** displays characteristic stretches for both the carbonyl (1691 cm^{-1}) and N–H (3389 cm^{-1}) functionalities.

X-ray diffraction analysis of a single crystal of **(Ar*NH)$_2$CO** (Figure 1), grown from a 1:1:5 THF/toluene/pentane solution over several days at −27 °C, unambiguously established composition and connectivity. **(Ar*NH)$_2$CO** crystallizes in the orthorhombic space group *Fdd*2 and lies on a crystallographic special position whereby half of the molecule is generated by inversion symmetry, showing the urea to adopt an overall E_{syn} conformation in the solid state.[15] In the solid-state molecular structure, the pendant aniline groups are observed to skew away from one another, forming a 72° dihedral angle between the mean planes of the aniline rings. The C1–N1–

dx.doi.org/10.1021/ic501219q | Inorg. Chem. 2014, 53, 8155–8164

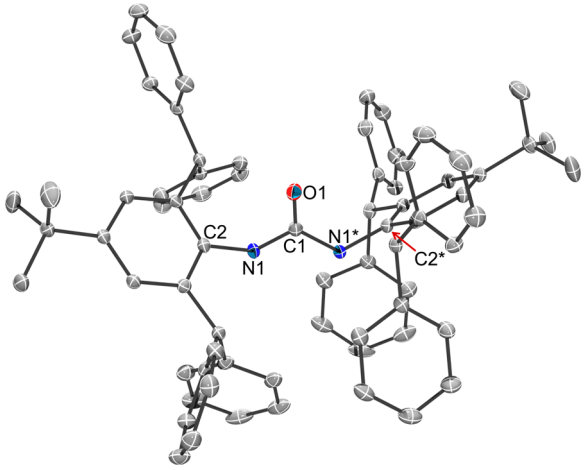

Figure 1. ORTEP diagram of $(\mathbf{Ar^*NH})_2\mathbf{CO}$ with 35% probability ellipsoids and hydrogen atoms omitted for clarity. Asterisks indicate symmetry-related atoms. Selected bond lengths (Å) and angles (deg): C1−O1 = 1.214(3), C1−N1 = 1.371(2), N1−C1−N1* = 113.1(2).

C1* angle of 113.1(2)° in $(\mathbf{Ar^*NH})_2\mathbf{CO}$ is unremarkable and similar to that found in less cumbersome, symmetrical aryl ureas, e.g., $(PhNH)_2CO$ (N−C−N = 113.6°).[16]

The urea $(\mathbf{Ar^*NH})_2\mathbf{CO}$ is readily dehydrated by its addition to a vigorously stirring slurry of P_2O_5/Al_2O_3 in pyridine with heating at 115 °C for 48 h.[17] Upon filtration and removal of the solvent under reduced pressure, the carbodiimide $(\mathbf{Ar^*N})_2\mathbf{C}$ is cleanly obtained in 81% yield (eq 3) as a colorless, air-stable

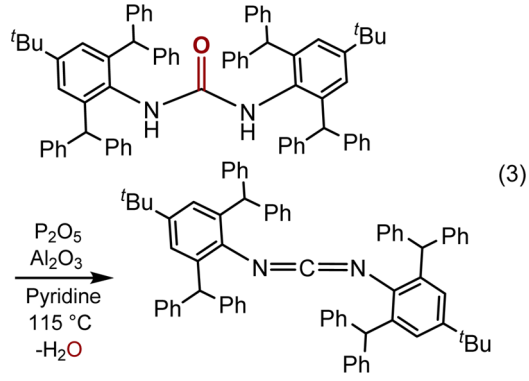

(3)

$(\mathbf{Ar^*N})_2\mathbf{C}$

solid. $(\mathbf{Ar^*N})_2\mathbf{C}$ is sparingly soluble in hexane but highly soluble in aromatic solvents and $CHCl_3$. Its ^1H NMR spectrum in C_6D_6 displays two sharp resonances at 1.09 and 6.06 ppm in an 18:4 ratio, attributable to the *tert*-butyl and methine protons, respectively. Furthermore, a distinctive resonance is observed in the $^{13}C\{^1H\}$ NMR spectrum at 146.9 ppm corresponding to the central carbon atom of the carbodiimide NCN moiety.

Single crystals of $(\mathbf{Ar^*N})_2\mathbf{C}$ were grown as colorless plates from the slow evaporation of a dilute $CHCl_3$ solution, open to air, over the course of 10 days at room temperature. $(\mathbf{Ar^*N})_2\mathbf{C}$ crystallizes in the triclinic space group $P\bar{1}$ and contains two independent half-molecules in its asymmetric unit, each with their central carbodiimide carbon atom positioned on a crystallographic inversion center. The two molecules possess near-identical metrical parameters, and the molecular structure of one full molecule, generated by symmetry, is shown in Figure 2. In the solid state, $(\mathbf{Ar^*N})_2\mathbf{C}$ adopts a *trans* configuration,

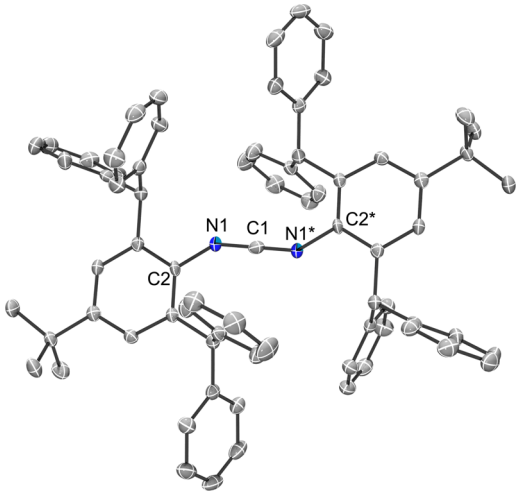

Figure 2. ORTEP diagram of $(\mathbf{Ar^*N})_2\mathbf{C}$ with 45% probability ellipsoids and hydrogen atoms omitted for clarity. Asterisks indicate symmetry-related atoms. Selected bond lengths (Å) and angles (deg): C1−N1 = 1.205(2), N1−C1−N1* = 180.0, C1−N1−C2 = 143.7(2), C2−N1−N1*−C2* = 180.0.

with its aniline rings positioned in a coplanar orientation. Interestingly, the linear heteroallene N−C−N angle (N1−C1−N1* = 180.0°) in $(\mathbf{Ar^*N})_2\mathbf{C}$ is atypical of carbodiimides, which normally exhibit slightly bent N−C−N angles, e.g., $(ArN)_2C$ [Ar = 2,6-diisopropylphenyl, N−C−N = 167.8(2)°; Ar = mesityl, N−C−N = 169.3(2)°],[18] while the carbodiimide N−C bond length [N1−C1 = 1.205(2) Å] of $(\mathbf{Ar^*N})_2\mathbf{C}$ is unexceptional and comparable to that of other aryl carbodiimides, e.g., $(ArN)_2C$ [Ar = 2,6-diisopropylphenyl, N−C = 1.213(2) Å; Ar = mesityl, N−C = 1.211(2) Å].[18a]

Gratifyingly, the addition of the nucleophile $LiN{=}C(^tBu)_2$ to $(\mathbf{Ar^*N})_2\mathbf{C}$ in a THF mixture with heating at 65 °C for 1 day smoothly generates the lithium guanidinate $\mathbf{Li}[^{Ar}\mathbf{*ketguan}]$ (Scheme 1). This reaction can be performed on a multigram scale, producing material in up to 85% yield. $\mathbf{Li}[^{Ar}\mathbf{*ketguan}]$ is a white solid that is partially soluble in aliphatics and highly soluble in aromatic and ethereal solvents. The ^1H NMR spectrum of $\mathbf{Li}[^{Ar}\mathbf{*ketguan}]$ in C_6D_6 exhibits two resonances at 1.34 and 1.09 ppm, corresponding to the *tert*-butyl protons of the aniline and ketimine substituents, while the methine proton of the diphenylmethyl groups appears at 6.12 ppm, overall indicative of C_{2v} geometry in solution. True to this, the phenyl rings of the diphenylmethyl groups are observed to be diastereotopic because the signals of their hydrogen atoms appear in the ^1H NMR spectrum as two sets of resonances consisting of one ill-resolved multiplet at 6.74 ppm and a set of signals at 7.08, 7.20, and 7.35 ppm (identified as *para*, *meta*, and *ortho* protons) in a total 20:4:8:8 ratio, respectively. Moreover, the $^{13}C\{^1H\}$ NMR spectrum of $\mathbf{Li}[^{Ar}\mathbf{*ketguan}]$ displays 12 aryl resonances, 8 from the diastereotopic phenyl rings of the diphenylmethyls and 4 from the *N*-aryl carbon atoms. The $^{13}C\{^1H\}$ NMR spectrum shows a diagnostic downfield resonance at 155.7 ppm for the central sp^2-hybridized carbon atom (C_{cent}) of the guanidine framework,[15] while the $^7Li\{^1H\}$ NMR spectrum displays a single resonance at −2.84 ppm. It should be noted that while the synthesis of $\mathbf{Li}[^{Ar}\mathbf{*ketguan}]$ is conducted in the presence of THF, the NMR spectrum of the isolated crystalline material is found to be absent of THF solvent molecules.

dx.doi.org/10.1021/ic501219q | Inorg. Chem. 2014, 53, 8155−8164

Scheme 1. Synthesis of "Super Bulky" Guanidinates M[^{Ar*}ketguan] (M = H, Li, K, Cs)

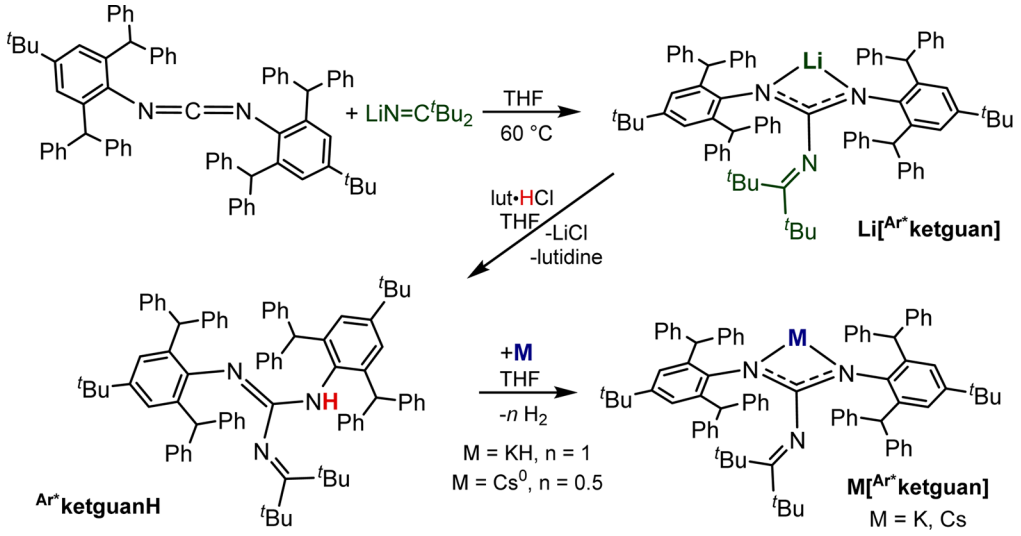

Li[^{Ar*}**ketguan**] is cleanly protonated by treatment with lutidinium chloride in THF to give ^{Ar*}**ketguanH** in nearly quantitative yield (Scheme 1), with the N−H proton of the guanidine appearing as a singlet at 4.75 ppm in the ^{1}H NMR spectrum. Furthermore, the ^{1}H NMR spectrum also displays two signals, accounting for nine protons each, at 1.10 and 1.16 ppm, attributable to the *tert*-butyl protons of the Ar*−amine and Ar*−imine functionalities of the guanidine, while the protons of the *tert*-butyl groups of the ketimine backbone appear as a sharp singlet at 0.74 ppm, integrating to an 18 proton ratio.

At room temperature, the ^{1}H NMR spectra of varying samples of ^{Ar*}**ketguanH** are always observed to exhibit a second set of minor broad peaks. Because guanidines are well-known to undergo dynamic conformational and tautomeric interconversion in solution,[15,19] we attribute these resonances to the presence of a minor isomer. Consistent with this, heating a solution of ^{Ar*}**ketguanH** in C_7H_8 to 50 °C increases the relative concentration of the minor isomer (Figure S15 in the Supporting Information, SI), while cooling to −50 °C appears to arrest fluxionality, resulting in its near disappearance (Figure S16 in the SI).

Highly soluble in aliphatic solvents, crystals of ^{Ar*}**ketguanH** can be grown from the storage of a concentrated hexane solution kept at −27 °C for several days. The composition of ^{Ar*}**ketguanH** was unequivocally confirmed by X-ray crystallographic analysis (see Figure S20 in the SI for atom connectivity), which shows it to adopt an E_{syn} conformation in the solid state; however, weak diffraction data preclude a meaningful discussion of its metrical parameters.

^{Ar*}**ketguanH** undergoes facile deprotonation to cleanly give the alkali salts **M**[^{Ar*}**ketguan**] (M = K, Cs) in 94% (K) and 51% (Cs)[20] yield as colorless solids, respectively (Scheme 1). Complexes **M**[^{Ar*}**ketguan**] (M = K, Cs) exhibit solubility properties comparable to those of their lithium counterparts, with the ^{1}H and ^{13}C{^{1}H} NMR spectra of all three alkali complexes appearing qualitatively similar, each distinguished by small, but significant, peak shifts.

Structural Comparison and Analyses. Molecular structure analyses were performed on **M**[^{Ar*}**ketguan**] (M = Li, K, Cs), representative of the alkali metal series, to understand the steric profile and coordination properties of the encumbering ligand scaffold, especially its ability to accommodate ions with covalent radii as small as Li^+ (1.28 Å) and as large as Cs^+ (2.44 Å).[21]

Various solvent combinations, stored at −25 °C, were used to grow crystals of **M**[^{Ar*}**ketguan**] (M = Li, K, Cs) suitable for X-ray diffraction analyses. Specifically, single crystals of **K**[^{Ar*}**ketguan**] were harvested from a concentrated hexane solution, while the lithium and cesium analogues were crystallized from hexane/THF and Et_2O/toluene mixtures, respectively. **M**[^{Ar*}**ketguan**] (M = Li, K) crystallize as the hexane solvates **M**[^{Ar*}**ketguan**]·$2C_6H_{14}$ [Figure 3, top (Li); Figure S29 in the SI (K)] in the monoclinic space group $P2_1$, whereas **Cs**[^{Ar*}**ketguan**] (Figure 3, bottom) crystallizes as an Et_2O solvate in the monoclinic space group $C2/c$, all possessing one full molecule in the crystallographic asymmetric unit.

The [^{Ar*}**ketguan**]$^-$ ligand ligates the alkali cations in a κ^2 fashion, with the metal centers "pinched" between the N_{Ar*} nitrogen atoms. Compared to other mononuclear complexes, the Li−N_{Ar*} distances in **Li**[^{Ar*}**ketguan**] [Li1−N1 = 2.131(3) Å; Li1−N2 = 2.189(3) Å] are found to be slightly longer than the those in [Li(THF)$_2$][(^{dipp}ArN)$_2$C(R)] [R = H; Li−N = 2.063(4) and 2.041(4) Å][22] or [Li(THF)$_2$][(^{dipp}ArN)$_2$C(*p*-tolyl)] [Li−N = 2.032(6) and 2.057(6) Å],[23] while the **K**[^{Ar*}**ketguan**] bond lengths [K1−N1 = 2.594(3) Å; K1−N2 = 2.896 Å] exhibit a greater range than those found for [K(18-crown-6)][hpp] [hpp = 1,3,4,6,7,8-hexahydro-2*H*-pyrimido-[1,2-*a*]pyrimidine; K−N = 2.82(1) and 2.73(1) Å].[24] A direct comparison of the M−N_{Ar*} bond lengths in **M**[^{Ar*}**ketguan**] (M = K, Cs) to other related systems is difficult because, to the best of our knowledge, no other structurally characterized monomeric K^+ or Cs^+ salts of the $[(ArN)_2C(R)]^-$ (R = H, CR_3, NR_2) type have been reported. The closest analogues for which a comparison can be made are the κ^2-triazenides M[N_3Tph$_2$] [M = K, Cs; Tph = 2-(2′,4′,6′-triisopropylphenyl)-biphenyl], which exhibit K−N_{Ar} distances [K−N = 2.709(1) and 2.723(1) Å] within the range found for **K**[^{Ar*}**ketguan**] [K1−N1 = 2.594(3) Å; K1−N2 = 2.896 Å] and Cs−N_{Ar} bond lengths [Cs−N = 3.065(5) and 3.071(4) Å] comparable or equivalent to those of **Cs**[^{Ar*}**ketguan**] [Cs1−N1 = 3.062(2) Å; Cs1−N2 = 2.939(2) Å].[25] Finally, it should be noted that the closely related amidinate K[$(ArN)_2C(^tBu)$] [Ar = 2,6-bis-

dx.doi.org/10.1021/ic501219q | *Inorg. Chem.* 2014, 53, 8155−8164

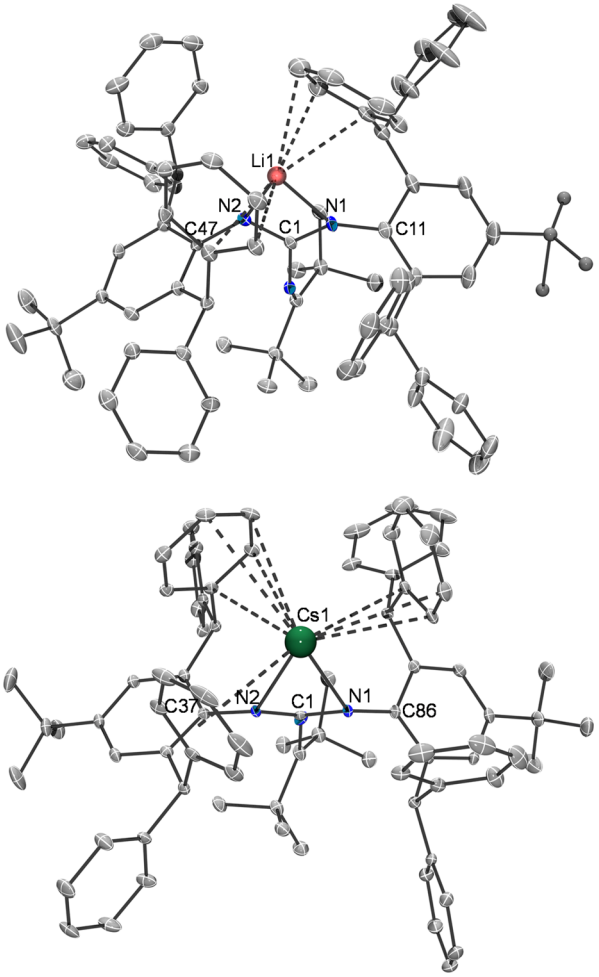

Figure 3. ORTEP diagrams of **Li**[^{Ar}***ketguan**] (top) and **Cs**[^{Ar}***ketguan**]·Et_2O (bottom) with 40% probability ellipsoids. Hydrogen atoms and the Et_2O solvent molecule are omitted for clarity. Selected bond lengths (Å) and angles (deg) for **Li**[^{Ar}***ketguan**]: Li1−N1 = 2.131(3), Li1−N2 = 2.189(3), C1−N1 = 1.334(2), C1−N2 = 1.320(2), N1−C1−N2 = 115.9(2), C1−N1−C11 = 120.8(2), C1−N2−C47 = 127.7(2). Selected bond lengths (Å) and angles (deg) for **Cs**[^{Ar}***ketguan**]·Et_2O: Cs1−N1 = 3.062(2), Cs1−N2 = 2.939(2), C1−N1 = 1.329(3), C1−N2 = 1.334(3), N1−C1−N2 = 117.5(2), C1−N1−C37 = 124.9(2), C1−N2−C86 = 120.9(2).

(diphenylmethyl)-4-methylphenyl] is known, but its solid-state structure has yet to be determined.[26]

The two N_{Ar*}−C_{cent} distances in **M**[^{Ar}***ketguan**] exist within a narrow range from C1−N2 = 1.302(2) Å in **Li**[^{Ar}***ketguan**] to C1−N2 = 1.334(3) Å in **Cs**[^{Ar}***ketguan**]. These N−C_{cent} distances are typical lengths for guanidinates and indicate charge delocalization across the diazaallyl unit.[15,23] Additionally, the N_{Ar*}−C_{cent}−N_{Ar*} angles [e.g., Li: N1−C1−N2 = 115.9(2)°] are unremarkable, while the C_{cent}−N_{Ar*}−C_{ipso} angles [e.g., Li: C1−N1−C11 = 120.8(2)° and C1−N2−C47 = 127.7(2)°] are comparable to the corresponding angles in other aryl guanidinates such as $[Li(^{dipp}ArN)_2C(NCy_2)]_2$ (C_{cent}−N_{dipp}−C_{ipso} = 119.3° and 125.8°).[27]

Notably, **M**[^{Ar}***ketguan**] (M = Li, K, Cs) do not aggregate in the solid state, as is common for alkali metals in guanidinates and their related amidinate and formamidinate counterparts,[12,25] with each **M**[^{Ar}***ketguan**] molecule existing as a distinct mononuclear species. Moreover, despite their synthesis in and recrystallization from ethereal solutions, namely THF, the metal centers are found to be free of coordinating solvents, consistent with their NMR spectra (vide supra). Indeed, this is clearly seen in **Cs**[^{Ar}***ketguan**], which cocrystallizes with a noncoordinating Et_2O molecule, although it should be noted that **Cs**[^{Ar}***ketguan**] does engage in a close neighbor interaction, via an intermolecular Cs−η^1-C_{arene} contact (Cs−C_{para} = 3.68 Å), forming an infinite 1D extended structure in the solid state (see Figure S32 in the SI). These observations, in total, clearly indicate a sufficiently encumbering architecture for [^{Ar}***ketguan**]$^-$, the steric features of which successfully prevent the formation of multinuclear clusters.

Specifically, the ligand [^{Ar}***ketguan**]$^-$ inhibits aggregation by encapsulating the metal cations within a hydrophobic cavity, or coordination pocket, defined by three encircling phenyl rings in **M**[^{Ar}***ketguan**] (M = Li, K) and four phenyl rings in **Cs**[^{Ar}***ketguan**], one ring contributed by each of the diphenylmethyl substituents. While formally two-coordinate, the alkali cations are seen to interact with the arenes that define the coordination pocket, forming secondary cation−π interactions, as determined by examination of the M−C_{arene} distances.[28] As may be anticipated, the number of metal−arene contacts in **M**[^{Ar}***ketguan**] correlates with the ion size, from η^2:η^3 for lithium to η^6:η^6 for potassium to η^3:η^4/η^6 for cesium. Additionally, the potassium cation in **K**[^{Ar}***ketguan**] exhibits a weak, long-distance interaction with the third ring of its coordination pocket (K−$C_{centroid}$ = 3.13 Å). However, as glimpsed from the solid-state structures of **M**[^{Ar}***ketguan**], ionic radii alone do not solely account for the varying range of metal−arene contacts. Interestingly, the size and shape of the coordination cavity is not uniform throughout the complexes but varies per cation, thus also having an effect on the metal−arene distances.

To better understand this structural phenomenon, a thorough comparison of the **M**[^{Ar}***ketguan**] (M = Li, K, Cs) solid-state structures, summarized in Table 1, was performed to assess the origin of the geometric differences between the metal complexes. Inspection of the dihedral angle formed between the aniline ring planes shows it to be very little changed between the complexes, varying from 45.9° (K) to 48.4° (Cs), indicating that twisting of the aniline rings, about the two N_{Ar*}−C_{ipso} axes, does not play a major role with respect to the shape or size of the coordination pocket. In contrast, the aniline groups do swivel out from the N_{Ar*}−C_{cent}−N_{Ar*} plane (as measured by the angle between the N_{Ar*}−C_{ipso} bond and the N_{Ar*}−C_{cent}−N_{Ar*} plane), which directly effects the positioning of the peripheral diphenylmethyl substituents and thus the size of the ligand cavity. For **M**[^{Ar}***ketguan**] (M = Li, K), the pendant anilines are each seen to swivel slightly away from the N_{Ar*}−C_{cent}−N_{Ar*} plane [Li: 15.2(1)°, 18.0(1)°; K: 10.9(3)°, and 15.2(3)°], consequently constricting the cavity boundary to a phenyl ring triad. In **Cs**[^{Ar}***ketguan**], the N_{Ar*}−C_{ipso} bonds deviate only marginally from the N_{Ar*}−C_{cent}−N_{Ar*} plane [Cs: 1.6(2)° and 2.9(2)°], resulting in a quadrilaterally shaped coordination pocket. Moreover, as seen from the $^{Ar*N}C_{ipso}$−C_{ortho}−$C_{methine}$−C_{ipso} torsion angles (Table 1), the diphenylmethyl groups can tilt inward toward a metal as with **M**[^{Ar}***ketguan**] (M = Li, K) [Li, 66.9° (avg); K, 68.0° (avg)] or outward as with **Cs**[^{Ar}***ketguan**] [Cs: 73.5° (avg)]. It must also be noted that the phenyl rings of the cavity can individually rotate. A structural overlay (Figure S25 in the SI) reveals **M**[^{Ar}***ketguan**] (M = Li, K) to be nearly superimposable with one key difference; relative to **K**[^{Ar}***ketguan**], one of the encircling phenyl rings rotates toward the Li^+ cation in

dx.doi.org/10.1021/ic501219q | Inorg. Chem. 2014, 53, 8155−8164

Table 1. Selected Metrical Parameters for [^{Ar*}ketguan]M (M = Li, K, Cs)

	M		
	Li	K	Cs
covalent radii[a] (Å)	1.28	2.03	2.44
M–N_{Ar*} (Å)	2.131(3), 2.189(3)	2.594(3), 2.896(3)	2.939(2), 3.062(2)
C_{cent}–N_{Ar*} (Å)[b]	1.320(2), 1.334(2)	1.324(5), 1.332(5)	1.329(3), 1.334(3)
N_{Ar*}–C_{cent}–N_{Ar*} (deg)	115.9(2)	118.2(3)	117.5(2)
N_{Ar*}–M–N_{Ar*} (deg)	59.9(1)	48.69(9)	44.54(5)
C_{cent}–N_{Ar*}–C_{ipso} (deg)	120.8(2), 127.7(2)	123.9(3), 127.9(3)	120.9(2), 124.9(2)
N_{Ar*}–N_{Ar*} ring planes dihedral (deg)	47.5	45.9	48.4
M displacement from N_{Ar*}–C_{cent}–N_{Ar*} plane (Å)	0.4	0.2	1.25
N_{Ar*}–C_{ipso} bond deviation from N_{Ar*}–C_{cent}–N_{Ar*} plane (deg)	15.2(1), 18.0(1)	10.9(3), 15.2(3)	1.6(2), 2.9(2)
C_{ipso}–C_{ortho}–$C_{methine}$–C_{ipso}[c]	56.9(2), 65.1(2), 70.7(2), 74.7(2)	60.9(5), 66.5(5), 68.6(5), 75.8(5)	66.6(3), 71.2(2), 77.4(3), 78.6(3)
metal–arene interactions and M–C distances (Å)	η^2, 2.604(3)–2.699(3); η^3, 2.484(4)–2.776(4)	η^6, 3.101(4)–3.284(5); η^6, 3.035(4)–3.327(4)	η^3, 3.407(3)–3.584(3); η^4, 3.509(3)–3.776(3); η^6, 3.628(3)–3.720(3)
% V_{Bur}[d]	94.8	92.1	81.7

[a]See ref 21. [b]C_{cent} refers to the central sp^2-hybridized C of the guanidine N_3C core. [c]Torsion angles involving phenyl rings within, or in proximity to, the metal's primary and secondary coordination spheres. [d]See ref 29 for the % V_{Bur} method of calculation.

Li[^{Ar*}**ketguan**], likely to increase the metal–arene contact with the smaller ion. Last, the metals themselves are not locked into the ligand coordination plane. As best exemplified in **Cs**[^{Ar*}**ketguan**], the Cs^+ cation is displaced 1.25 Å from the guanidinate N_{Ar*}–C_{cent}–N_{Ar*} plane. In summary, the geometric components of [^{Ar*}**ketguan**]$^-$ provide several pivot points, affording multiple degrees of freedom that yield an encapsulating, but remarkably flexible, ligand scaffold.

Steric Measures. Finally, to quantitatively assess the steric demand of the ligand (utilizing the solid-state conformations found for each of the metal complexes in **M**[^{Ar*}**ketguan**]), Samb*V*ca calculation analyses were performed to determine the percent buried volumes (%V_{Bur}).[29] Percent buried volumes are most often applied to NHCs to describe their steric profile, with the bulkiest NHC to date being the bis[2,6-(dinaphthylmethyl)phenyl]-functionalized IPr*$^{(2\text{-Np})}$ possessing a 57.1% V_{Bur}.[10b] In **Li**[^{Ar*}**ketguan**], the Li^+ cation is almost entirely engulfed by the ligand with a 94.8% V_{Bur}, which is graphically represented by the space-filling models shown in Figure 4. The K^+ cation in **K**[^{Ar*}**ketguan**] is only slightly more exposed at 92.1% V_{Bur}, while the Cs^+ cation is significantly more accessible with a 81.7% V_{Bur} (Figure 4). This accessibility to Cs^+ likely permits the intermolecular Cs–C_{arene} interaction, which is observed to occur in **Cs**[^{Ar*}**ketguan**]·Et_2O (vide supra).

As generally compared to other sterically hindering aryl guanidinates, such as $[(^{dipp}ArN)_2C(NMe_2)]^-$ for lithium (51.7% V_{Bur})[30] or $[(^{dipp}ArN)_2C(N^iPr_2)]^-$ for calcium (51.9% V_{Bur}) and strontium (52.8% V_{Bur}),[31] their buried volumes are significantly less encumbering relative to [^{Ar*}**ketguan**]$^-$. Furthermore, the terphenyl-backbone-functionalized amidinate [dimb]$^-$ [dimb = *N*,*N*′-diisopropyl(2,6-dimesityl)-benzamidinate] exhibits 49.4% V_{Bur} on magnesium,[19a] while the diadamantylaluminum amidinate $[(NAd)_2C^tBu]^-$ possesses 53.0% V_{Bur}.[32] The upper range for % V_{Bur} of the bulky triazenides M[N_3Tph_2] [M = Li (47.1% V_{Bur}), K (83.2% V_{Bur}), Cs (76.0% V_{Bur})] is comparable to that observed for **Cs**[^{Ar*}**ketguan**] but exhibits greater % V_{Bur} variability, leading to the formation of aggregated lithium species $\{Li[N_3Tph_2]\}_2$ at the lower end of the range.[25] Clearly, [^{Ar*}**ketguan**]$^-$ stands apart, especially from other hindered guanidinates or amidinates, and is best described as an exceedingly encumbering, or "super bulky", ligand platform.

SUMMARY

We have presented the synthesis of the new "super bulky" and encapsulating guanidinate [^{Ar*}**ketguan**]$^-$, which can be readily synthesized in four steps on multigram scales utilizing an easily prepared 2,6-bis(diphenylmethyl)-4-*tert*-butylaniline precursor. The [^{Ar*}**ketguan**]$^-$ ligand is able to coordinate metal ions of various sizes from Li^+ to Cs^+ in a typical guanidinate κ^2 fashion, giving formally two-coordinate metal centers while also preventing the formation of aggregated alkali metal clusters. Inspection of the solid-state structures of **M**[^{Ar*}**ketguan**] (M = Li, K, Cs) shows that the alkali cations sit within a cavity formed from the peripheral phenyl rings of the diphenylmethyl substituents, which also provide additional support to the cations via intramolecular metal–arene interactions. Moreover, close examination of the ligand framework and its geometric properties reveals a highly flexible ligand architecture that accommodates the disparately sized ions via an expandable coordination pocket. Samb*V*ca calculations were used to quantify the steric properties of [^{Ar*}**ketguan**]$^-$, which show large % V_{Bur} values [94.8% V_{Bur} (Li), 92.1% V_{Bur} (K), 81.8%

dx.doi.org/10.1021/ic501219q | Inorg. Chem. 2014, 53, 8155–8164

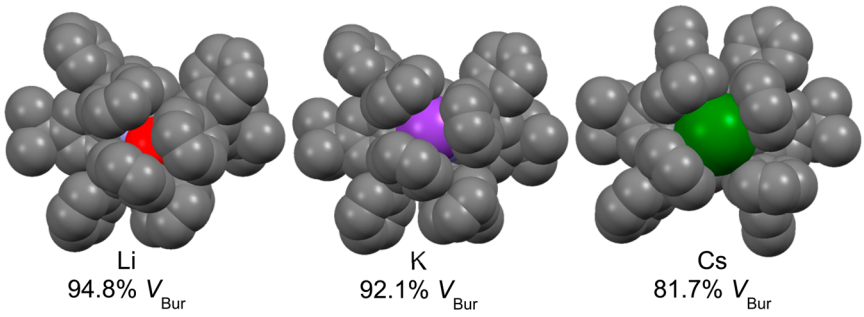

Figure 4. Space-filling models and percent buried volumes for (% V_{Bur}) for **M**[**Ar*ketguan**] (M = Li, K, Cs). Gray, red, purple, and green spheres represent carbon, lithium, potassium, and cesium atoms, respectively.

V_{Bur} (Cs)] significantly greater than those of other sterically hindering guanidinates and amidinates. Notably, while highly encumbered, the % V_{Bur} values indicate that the alkali metal cations are not entirely buried and do remain exposed; thus, we expect that the reactivity of these salts will not be completely averted. As such, we are currently examining the chemistry of the **M**[**Ar*ketguan**] (M = Li, K, Cs) salts in metathetic reactions with other metal halides.

EXPERIMENTAL SECTION

General Considerations. All air- and moisture-sensitive operations were performed in an M. Braun drybox under an atmosphere of purified nitrogen or using high-vacuum standard Schlenk techniques. Diethyl ether, hexanes, pentanes, toluene, and THF were dried using a Pure Process Technology Solvent Purification System and subsequently stored under a dinitrogen atmosphere over activated 4 Å molecular sieves. Pyridine was distilled from calcium hydride. All deuterated solvents were purchased from Cambridge Isotope Laboratories Inc., degassed by three freeze−pump−thaw cycles, and dried over activated 4 Å molecular sieves for 24 h prior to use. Celite, alumina, and 4 Å molecular sieves were heated to 150 °C for at least 24 h and then cooled under vacuum. LiN=C^{t}Bu[33] and anhydrous lutidinium chloride[34] were prepared following literature procedures, while all other reagents were purchased from commercial suppliers and used as received. NMR spectra were recorded on a JEOL ECA 600 MHz or a Bruker AVANCE III 400 MHz spectrometer. ^{1}H NMR and ^{13}C NMR spectra are referenced to $SiMe_4$ using the residual ^{1}H solvent peaks as internal standards or the characteristic ^{13}C resonances of the solvent. ^{7}Li{^{1}H} spectra were referenced to external LiCl in D_2O. Mass spectrometry (MS) analyses were conducted using a JEOL AccuTOF JMS-T100LC or a Bruker MALDI-TOF Microflex mass spectrometer. IR data were collected using the attenuated total reflectance (ATR) method on a PerkinElmer Spectrum 100 Fourier transform infrared (FTIR) spectrometer.

Synthesis of Ar*NH$_2$. To a 500 mL round-bottomed flask equipped with a large stir bar was added benzhydrol (61.75 g, 0.34 mol) and 4-*tert*-butylaniline (26.7 mL, 0.17 mol). The mixture was vigorously stirred with heating to 125 °C for 1 h, resulting in the formation of a homogeneous, light-pink melt. A solution of $ZnBr_2$ (20.24 g, 0.09 mol) in HCl (14 mL, 0.18 mol, 12.1 M) was added dropwise, which was observed to fill the headspace of the flask with white fumes. The reaction mixture was stirred with heating for 0.5 h, at which point the material solidified into a glassy solid, which was subsequently heated without stirring for an additional 2.5 h at 125 °C. Upon cooling to room temperature, the solid was dissolved in $CHCl_3$ (300 mL) and washed with a saturated solution of NH_4Cl followed by two washings with brine. The resulting light-brown solution was dried of excess water with anhydrous $MgSO_4$ and subsequently filtered through a Büchner funnel to remove the solids. $CHCl_3$ was removed under reduced pressure, giving an off-white solid. The product was washed copiously with MeOH, producing pure material as a white powder. Yield: 66.7 g, 80%. ^{1}H NMR (25 °C, 600 MHz, $CDCl_3$): δ 0.98 (s, 9H, CCH_3), 3.28 (s, 2H, NH_2), 5.47 (s, 2H, CHPh$_2$), 6.58 (s, 2H, *m*-CH *N*-aryl), 7.10 (d, 8H, J_{HH} = 7.34 Hz, *o*-CH aryl), 7.22 (t, 4H, J_{HH} = 7.32 Hz, *p*-CH aryl), 7.29 (t, 8H, J_{HH} = 7.53 Hz, *m*-CH aryl). ^{13}C{^{1}H} NMR (25 °C, 100.58 MHz, $CDCl_3$): δ 31.4 (CCH_3), 34.0 (CCH_3), 52.8 (CPh_2), 125.6 (aryl), 126.6 (aryl), 128.5 (aryl), 128.6 (aryl), 129.6 (aryl), 139.6 (aryl), 140.1 (aryl), 143.0 (aryl). IR (ATR, ZnSe crystal, cm^{-1}): 3421 (w, ν_{asym} NH_2), 3360 (w, ν_{sym} NH_2), 3087 (w), 3025 (w), 2962 (m), 2892 (m), 2858 (w), 1627 (m), 1601 (m), 1493 (m), 1473 (m), 1447 (m), 1427 (w), 1391 (m), 1361 (m), 1342 (w), 1304 (w), 1296 (m), 1273 (m), 1244 (m), 1186 (m), 1158 (w), 1141 (w), 1119 (w), 1077 (m), 1031 (m), 1005 (w), 970 (w), 946 (w), 924 (w), 912 (m), 892 (m), 865 (w), 835 (w), 760 (s), 736 (s), 697 (s) 661 (s). MALDI-TOF-MS (THA matrix): *m*/*z* 481.18 ([M]$^+$; calcd *m*/*z* 481.28).

Synthesis of (Ar*NH)$_2$CO. To a 500 mL heavy-walled pressure vessel equipped with a large stir bar was added **Ar*NH$_2$** (33.08 g, 0.07 mol) and DMAP (8.47g, 0.07 mol) into CH_2Cl_2 (250 mL). The solution was cooled to −78 °C, and triphosgene (3.40 g, 0.01 mol) was added as a solid with stirring. The pressure vessel was immediately sealed, and the reaction mixture was allowed to warm to room temperature, forming a white slurry. The slurry was subsequently heated at 60 °C for 15 days, upon which time the solution turned clear and colorless. Upon recooling to room temperature, the solution was washed with water (200 mL × 2) and dried with $MgSO_4$. The mixture was filtered through a Büchner funnel and the CH_2Cl_2 was removed under reduced pressure to give a yellow oil. The oil was triturated with hexanes (250 mL), causing precipitation of a white solid. The solid was isolated on a Büchner funnel, giving the product as a pure white powder. Yield: 29.3 g, 86%. ^{1}H NMR (25 °C, 600 MHz, C_6D_6): δ 1.05 (s, 18H, CCH_3), 4.55 (s, 2H, NH), 6.31 (s, 4H, CHPh$_2$), 6.99 (m, 8H, J_{HH} = 7.32 Hz, CH aryl), 7.07 (m, 16H, J_{HH} = 7.58 Hz, CH aryl), 7.21 (s, 4H, *m*-CH *N*-aryl), 7.38 (br s, 16H, CH aryl, fwhm = 100 Hz). ^{13}C{^{1}H} NMR (25 °C, 151 MHz, C_6D_6): δ 31.2 (CCH_3), 34.7 (CCH_3), 52.7 (CPh_2), 126.6 (aryl), 126.6 (aryl), 128.3 (aryl), 128.6 (aryl), 130.0 (aryl), 132.5 (aryl), 142.9 (aryl), 150.1 (aryl), 154.7 (*C*=O). IR (ATR, ZnSe crystal, cm^{-1}): 3389 (w, ν NH), 3086 (w), 3059 (w), 3027 (w), 2955 (m), 2921 (w), 2863 (w), 1691 (s, ν CO), 1599 (m), 1580 (w), 1494 (s), 1446 (s), 1414 (m), 1395 (w), 1363 (m), 1293 (w), 1275 (w), 1258 (w), 1214 (s), 1190 (w), 1177 (w), 1078 (m), 1030 (m), 1002 (w), 948 (w), 920 (w), 896 (w), 766 (s), 734 (s), 699 (s). ESI-MS: *m*/*z* 989.53 ([M + H]$^+$; calcd *m*/*z* 989.54).

Synthesis of (Ar*N)$_2$C. To a 500 mL heavy-walled pressure vessel equipped with a large stir bar was added **(Ar*NH)$_2$CO** (12.1 g, 12.2 mmol), P_2O_5 (17.3 g, 122 mmol), Al_2O_3 (12.4 g, 122 mmol), and pyridine (150 mL). The vessel was tightly sealed under an atmosphere of N_2, and the reaction mixture was stirred at 115 °C, forming a thick white slurry after 30 min. After 2 days, the mixture was filtered in air through a 350 mL medium-porosity glass frit, and the solids were thoroughly washed with toluene (100 mL). The filtrate was dried under reduced pressure using a rotary evaporator, yielding a white powder. Yield: 9.6 g, 81%. ^{1}H NMR (25 °C, 600 MHz, C_6D_6): δ 1.09 (s, 18H, CCH_3), 6.06 (s, 4H, CHPh$_2$), 7.00−7.03 (m, 8H, CH aryl), 7.07−7.11 (m, 32H, CH aryl), 7.20 (s, 4H, *m*-CH *N*-aryl). ^{13}C{^{1}H} NMR (25 °C, 151 MHz, C_6D_6): δ 31.2 (CCH_3), 34.6 (CCH_3), 53.0 (CPh_2), 126.3 (aryl), 126.6 (aryl), 128.3 (aryl), 128.5 (aryl), 130.0

dx.doi.org/10.1021/ic501219q | *Inorg. Chem.* 2014, 53, 8155−8164

(aryl), 132.9 (aryl), 139.1 (aryl), 143.9 (aryl), 146.8 (NCN). IR (ATR, ZnSe crystal, cm^{-1}): 3084 (w), 3064 (w), 3027 (w), 2969 (w), 2870 (w), 2236 (s), 1693 (w), 1598 (w), 1593 (w), 1565 (w), 1493 (m), 1487 (w), 1444 (m), 1414 (w), 1394 (w), 1364 (w), 1292 (w), 1254 (m), 1181 (m), 1156 (w), 1114 (w), 1075 (m), 1031 (m), 971 (w), 947 (w), 913 (w), 895 (w), 862 (w), 834 (w), 766 (m), 753 (m), 736 (m), 696 (s), 668 (m). MALDI-TOF-MS (THA matrix): m/z 970.59 ($[M]^+$; calcd m/z 970.52), 971.59 ($[M + H]^+$; calcd m/z 971.53).

Synthesis of Li[^{Ar}*ketguan]. To a 100 mL Cajon flask, containing a small stir bar, was added **(Ar*N)$_2$C** (8.7 g, 8.9 mmol), LiNC(^{t}Bu)$_2$ (1.54 g, 10.5 mmol), and THF (80 mL). The reaction mixture was stirred at 65 °C for 1 day, during which time the color of the solution turned from light to deep yellow. After 1 day, the volatiles were removed under reduced pressure to afford a light-yellow powder, which was subsequently washed with cold hexane (20 mL, −25 °C) to give pure product as an off-white powder. Yield: 8.5 g, 85%. ^{1}H NMR (25 °C, 400 MHz, C_6D_6): δ 1.09 (s, 18H, CCH_3), 1.34 (s, 18H, CCH_3), 6.12 (s, 4H, CHPh$_2$), 6.74 (br m, 20H, CH aryl, fwhm = 12 Hz), 6.91 (s, 4H, *m*-CH *N*-aryl), 7.08 (t, 4H, J_{HH} = 7.34 Hz, *p*-CH aryl), 7.20 (t, 8H, J_{HH} = 7.68 Hz, *m*-CH aryl), 7.35 (d, 8H, J_{HH} = 7.34 Hz, *o*-CH aryl). ^{13}C{^{1}H} NMR (25 °C, 101 MHz, C_6D_6): δ 30.7 (CCH_3), 31.5 (CCH_3), 34.4 (CCH_3), 43.8 (CCH_3), 53.5 (CPh_2), 125.5 (aryl), 126.3(aryl), 126.3 (aryl), 128.5 (aryl), 128.8 (aryl), 130.6 (aryl), 139.0 (aryl), 142.4 (aryl), 145.4 (aryl), 146.3 (aryl), 146.5 (aryl), 155.7 (NCN_2), 172.6 (NC^tBu$_2$), with one aryl carbon resonance not observed. ^{7}Li{^{1}H} NMR (25 °C, 155 MHz, C_6D_6): δ −2.84. IR (ATR, ZnSe crystal, cm^{-1}): 3085 (w), 3061 (w), 3025 (w), 2957 (m), 2901 (w), 2864 (w), 1662 (m), 1600 (m), 1494 (m), 1474 (m), 1431 (s), 1384 (m), 1362 (m), 1286 (w), 1241 (m), 1184 (w), 1155 (w), 1076 (m), 1046 (w), 1032 (m), 967 (m), 911 (w), 891 (w), 867 (w), 766 (m), 736 (m), 700 (s), 678 (m). Anal. Calcd $C_{82}H_{84}LiN_3$: C, 88.05; H, 7.57; N, 3.76. Found: C, 87.95; H, 7.67; N, 3.89.

Synthesis of ^{Ar}*ketguanH. To a 100 mL round-bottomed flask containing a small stir bar was added **Li[^{Ar}*ketguan]** (2.7 g, 2.4 mmol), lutidinium chloride (0.38 g, 2.64 mmol), and THF (20 mL). The colorless reaction mixture was stirred at room temperature under an dinitrogen atmosphere for 1 day and was subsequently filtered through Celite supported on a medium-porosity glass frit. The volatiles of the filtrate were removed in vacuo to afford a colorless paste. To this was added toluene (10 mL), and the solution was again filtered. The solvent of the filtrate was removed under reduced pressure. The material was subsequently dissolved in hexane (10 mL) and refiltered. The hexane solvent was then removed in vacuo to cleanly give the product as a white solid. Yield: 2.5 g, 97%. ^{1}H NMR (25 °C, 400 MHz, C_6D_6): δ 0.74 (s, 18H, CCH_3), 1.04 (s, minor isomer), 1.10 (s, 9H, CCH_3), 1.16 (s, 9H, CCH_3), 4.75 (s, 1H, NH), 5.75 (br s, fwhm = 22 Hz, minor isomer), 5.99 (s, minor isomer), 6.31 (s, minor isomer), 6.32 (s, 2H, CHPh$_2$), 6.69 (s, 1H, CHPh$_2$), 6.70 (s, 1H, CHPh$_2$), 6.76−7.57 (m, minor isomer), 6.93−7.19 (m, 34H, CH aryl), 7.25 (t, 4H, J_{HH} = 7.66 Hz, CH aryl), 7.28 (s, 2H, *m*-CH *N*-aryl), 7.56 (d, 4H, J_{HH} = 7.64 Hz, CH aryl). ^{13}C{^{1}H} NMR (25 °C, 101 MHz, C_6D_6): δ 30.2 (CCH_3), 31.4 (CCH_3), 31.5 (CCH_3), 34.4 (CCH_3), 34.7 (CCH_3), 43.4 (CCH_3), 52.8 (CPh_2), 53.1 (CPh_2), 125.3 (aryl), 125.8 (aryl), 126.2 (aryl), 126.3 (aryl), 126.6 (aryl), 127.0 (aryl), 128.1 (aryl), 127.9 (aryl), 128.4 (aryl), 128.7 (aryl), 129.6 (aryl), 129.7 (aryl), 130.8 (aryl), 130.9 (aryl), 135.3 (aryl), 136.2 (aryl), 141.7 (aryl), 143.3 (aryl), 143.8 (aryl), 145.0 (aryl), 145.5 (aryl), 146.2 (aryl), 146.3 (aryl), 149.0 (aryl), 150.1 (NCN_2), 179.6 (NC^tBu$_2$). ^{1}H NMR (−50 °C, 600 MHz, C_7D_8): δ 0.64 (br s, 18H, CCH_3, fwhm = 40 Hz), 1.12 (s, 9H, CCH_3), 1.19 (s, 9H, CCH_3), 4.74 (s, 1H, NH), 6.31 (s, 2H, CHPh$_2$), 6.74 (br s, 2H, CHPh$_2$, fwhm = 70 Hz), 6.90−7.14 (m, 34H, CH aryl), 7.26 (t, 4H, J_{HH} = 7.52 Hz, CH aryl), 7.31 (s, 2H, *m*-CH *N*-aryl), 7.57 (d, 4H, J_{HH} = 7.58 Hz, CH aryl). ^{13}C{^{1}H} NMR (−50 °C, 151 MHz, C_7D_8): δ 30.3 (CCH_3), 31.4 (CCH_3), 31.5 (CCH_3), 34.4 (CCH_3), 34.7 (CCH_3), 43.4 (CCH_3), 52.8 (CPh_2), 53.1 (CPh_2), 125.4 (aryl), 125.7 (aryl), 126.1 (aryl), 126.2 (aryl), 126.6 (aryl), 127.0 (aryl), 128.1 (aryl), 128.3 (aryl), 128.6 (aryl), 129.1 (aryl), 129.6 (aryl), 129.8 (aryl), 130.8 (aryl), 130.9 (aryl), 135.4 (aryl), 136.2 (aryl), 141.8 (aryl), 143.2 (aryl), 143.9 (aryl), 145.0 (aryl), 145.6 (aryl), 145.9 (aryl), 146.4 (aryl), 148.9 (aryl), 150.0 (NCN), 179.7 (NC^tBu$_2$). IR (ATR, ZnSe crystal, cm^{-1}): 3403 (w, ν NH), 3081 (w), 3063 (w), 3027 (w), 2956 (m), 2922 (m), 2867 (m), 2236 (w), 1647 (m), 1617 (m), 1597 (m), 1494 (m), 1471 (m), 1446 (m), 1414 (w), 1394 (w), 1362 (w), 1300 (w), 1236 (m), 1205 (m), 1181 (m), 1116 (w), 1077 (m), 1047 (w), 1032 (m), 1024 (w), 971 (m), 948 (w), 918 (w), 895 (w), 865 (w), 840 (w), 763 (m), 741 (m), 713 (m), 697 (s). MALDI-TOF-MS (DCTB matrix): m/z 1112.71 ($[M + H]^+$; calcd m/z 1112.68).

Synthesis of K[^{Ar}*ketguan]. To a 100 mL round-bottomed flask containing a small stir bar fitted with a glass stopper was added **^{Ar}*ketguanH** (1.8 g, 1.6 mmol), potassium hydride (0.70 g, 1.75 mmol), and THF (20 mL). The glass stopper of the flask was occasionally removed to release the evolved hydrogen gas. After 1 day, the solution was filtered to remove excess potassium hydride through Celite supported on a medium-porosity glass frit. All volatiles were removed under reduced pressure to afford a colorless paste. To this was added hexane (10 mL), and the colorless solution was again filtered. The solvent of the filtrate was removed in vacuo to give a white solid. Yield: 1.7 g, 94%. ^{1}H NMR (25 °C, 400 MHz, C_6D_6): δ 1.10 (s, 18H, CCH_3), 1.34 (s, 18H, CCH_3), 6.27 (s, 4H, CHPh$_2$), 6.67 (t, 4H, J_{HH} = 7.24 Hz, *p*-CH aryl), 6.75 (t, 8H, J_{HH} = 7.45 Hz, *m*-CH aryl), 6.92 (s, 4H, *m*-CH *N*-aryl, overlapping with CH aryl), 6.93 (d, 8H, *o*-CH aryl, overlapping with CH *N*-aryl), 7.11 (t, 4H, J_{HH} = 7.35 Hz, *p*-CH aryl), 7.23 (t, 8H, J_{HH} = 7.66 Hz, *m*-CH aryl), 7.41 (d, 8H, J_{HH} = 7.42 Hz, *o*-CH aryl). ^{13}C{^{1}H} NMR (25 °C, 101 MHz, C_6D_6): δ 31.0 (CCH_3), 31.6 (CCH_3), 34.4 (CCH_3), 34.4 (CCH_3), 43.9 (CPh_2), 53.3 (CPh_2), 124.7 (aryl), 125.6 (aryl), 126.2 (aryl), 130.3 (aryl), 131.0 (aryl), 136.8 (aryl), 140.0 (aryl), 146.0 (aryl), 148.5 (aryl), 149.0 (aryl), 153.0 (NCN_2), 169.6 (NC^tBu$_2$), with two aryl carbon resonances not observed. IR (ATR, ZnSe crystal, cm^{-1}): 3082 (w), 3060 (w), 3025 (w), 2956 (m), 2929 (w), 2867 (w), 1659 (w), 1636 (w), 1604 (w), 1596 (m), 1492 (m), 1470 (m), 1444 (s), 1429 (s), 1385 (m), 1361 (m), 1288 (w), 1236 (m), 1181 (m), 1122 (w), 1075 (m), 1049 (w), 1032 (m), 968 (w), 949 (w), 910 (w), 890 (w), 859 (w), 768 (m), 735 (s), 698 (s), 672 (m). Anal. Calcd $C_{82}H_{84}KN_3$: C, 85.59; H, 7.36; N, 3.65. Found: C, 85.48; H, 7.36; N, 3.60.

Synthesis of Cs[^{Ar}*ketguan]. To a 20 mL scintillation vial containing a small stir bar was added cesium metal (0.028 g, 0.21 mmol), **^{Ar}*ketguanH** (0.202 g, 0.18 mmol), and THF (10 mL). The color of the solution instantly turned red-orange with stirring. After 2 h, the solvent was removed in vacuo to afford an orange solid, which was dissolved in a 10:1 toluene/diethyl ether solution (5 mL). Storage of the solution at −25 °C for 1 week produced light-orange crystals, which upon washing with cold (−25 °C) pentane (0.25 mL × 2) gave 0.1 g of **Cs[^{Ar}*ketguan]**·Et$_2$O as a colorless solid. Slow evaporation of the supernatant over several weeks provided an additional 20 mg of product. Yield: 0.120 g 51%. ^{1}H NMR (25 °C, 400 MHz, C_6D_6): δ 1.12 (t, 6H, β-Et$_2$O protons), 1.15 (s, 18H, CCH_3), 1.25 (s, 18H, CCH_3), 3.27 (q, 4H, α-Et$_2$O protons), 6.51 (s, 4H, CHPh$_2$), 6.69 (t, 4H, J_{HH} = 7.31 Hz, *p*-CH aryl), 6.82 (t, 8H, J_{HH} = 7.59 Hz, *m*-CH aryl), 7.09 (d, 4H, J_{HH} = 7.20 Hz, *o*-CH *N*-aryl), 7.12 (s, 4H, *m*-CH *N*-aryl, overlapping with *p*-CH aryl), 7.12 (t, 4H, *p*-CH aryl, overlapping with CH *N*-aryl), 7.25 (t, 8H, J_{HH} = 7.68 Hz, *m*-CH aryl), 7.51 (d, 8H, J_{HH} = 7.42 Hz, *o*-CH aryl). ^{13}C{^{1}H} NMR (25 °C, 101 MHz, C_6D_6): δ 15.6 (Et$_2$O), 31.1 (CCH_3), 31.7 (CCH_3), 34.4 (CCH_3), 43.7 (CCH_3), 53.5 (CPh_2), 124.9 (aryl), 125.2 (aryl), 126.2 (aryl), 127.9 (aryl), 128.2 (aryl), 130.7 (aryl), 131.3 (aryl), 136.5 (aryl), 140.2 (aryl), 145.7 (aryl), 149.8 (aryl), 149.9 (aryl), 170.1 (NC^tBu$_2$), with the NCN_2 guanidine carbon resonance not observed. Anal. Calcd $C_{82}H_{84}CsN_3$·$C_4H_{10}O$: C, 78.34; H, 7.19; N, 3.19. Found: C, 78.34; H, 7.24; N, 3.14.

X-ray Crystallography. Data for **(Ar*NH)$_2$CO**, **(Ar*N)$_2$C**, **Li[^{Ar}*ketguan]**, **K[^{Ar}*ketguan]**·2C_6H_{14}, and **Cs[^{Ar}*ketguan]**·Et$_2$O were collected on a Bruker 3-axis platform diffractometer equipped with a APEX I CCD detector using a graphite monochromator with a Mo Kα X-ray source (α = 0.71073 Å). The crystals were mounted on a glass fiber or on a Mitigen Kapton loop, coated in NVH oil, and maintained at 100(2) K under a flow of nitrogen gas during data collection. A hemisphere of data was collected using ω and φ scans with 0.3° frame widths. Data collection and cell parameter determination were conducted using the *SMART* program.[35]

dx.doi.org/10.1021/ic501219q | *Inorg. Chem.* 2014, 53, 8155−8164

Table 2. X-ray Crystallographic Data for Complexes $(Ar^*NH)_2CO$, $(Ar^*N)_2C$, Li[^{Ar}*ketguan], K[^{Ar}*ketguan]·$2C_6H_{14}$, and Cs[^{Ar}*ketguan]·Et_2O

	$(Ar^*NH)_2CO$	$(Ar^*N)_2C$	Li[^{Ar}*ketguan]	K[^{Ar}*ketguan]·$2C_6H_{14}$	Cs[^{Ar}*ketguan]·Et_2O
empirical formula	$C_{73}H_{68}NO$	$C_{73}H_{66}N_2$	$C_{82}H_{84}LiN_3$	$C_{82}H_{84}KN_3·2C_6H_{14}$	$C_{82}H_{84}CsN_3·Et_2O$
cryst habit, color	needle, colorless	plate, colorless	plate, colorless	plate, colorless	block, pale yellow
cryst size (mm)	0.19 × 0.10 × 0.04	0.28 × 0.23 × 0.09	0.24 × 0.22 × 0.05	0.08 × 0.05 × 0.02	0.20 × 0.17 × 0.17
cryst syst	orthorhombic	triclinic	monoclinic	monoclinic	monoclinic
space group	*Fdd*2	$P\bar{1}$	$P2_1$	$P2_1$	$C2/c$
volume (Å^3)	11244(2)	2739.5(4)	3876.6(7)	3939.3(1)	14380(2)
a (Å)	28.013(2)	11.516(1)	12.979(1)	13.3345(3)	47.125(3)
b (Å)	36.621(3)	13.946(1)	18.904(2)	19.1840(4)	13.7727(9)
c (Å)	10.3927(8)	18.861(2)	16.000(2)	15.6017(3)	22.174(1)
α (deg)	90	69.174(2)	90	90	90
β (deg)	90	80.489(2)	99.066(2)	100.092(1)	92.324(1)
γ (deg)	90	76.285(2)	90	90	90
Z	8	2	2	2	8
fw (g/mol)	989.29	971.41	1118.46	1322.97	1318.55
density (calcd) (Mg/m^3)	1.169	1.195	0.958	1.118	1.218
abs coeff (mm^{-1})	0.068	0.068	0.055	0.115	0.563
F_{000}	4224.0	1064.0	1200.0	1432.0	5552.0
total no. of reflns	22524	27105	42096	47462	78298
unique reflns	5751	10489	17151	13389	16603
final R indices [$I > 2\sigma(I)$]	R1 = 0.0394, wR2 = 0.0822	R1 = 0.0564, wR2 = 0.1467	R1 = 0.0536, wR2 = 0.1201	R1 = 0.0680, wR2 = 0.1570	R1 = 0.0376, wR2 = 0.1031
largest diff peak and hole (e/Å^3)	0.262 and −0.264	0.240 and −0.240	0.44 and −0.18	0.62 and −0.35	0.50 and −0.57
GOF	1.052	0.999	0.974	1.043	0.826

Integration of the data and final cell parameter refinements were performed using *SAINT* software,[36] with data absorption correction implemented through *SADABS*.[37] Structures were solved using direct, charge-flipping, or structure expansion methods and difference Fourier techniques. All hydrogen atom positions were idealized and rode on the atom of attachment, with exceptions noted in the subsequent paragraph. Structure solution, refinement, graphics, and creation of publication materials were performed using *SHELXTL*[38] or the *Olex2* crystallographic package.[39]

Complex **Li[^{Ar}*ketguan]** cocrystallizes with two hexane molecules that exhibit severe crystallographic disorder. Attempts to model the solvent disorder were unsuccessful, resulting in a high wR2 refinement value. The *Olex2* solvent masking procedure[39] gave significant improvement in the data statistics. Addtionally, **Li[^{Ar}*ketguan]** and **K[^{Ar}*ketguan]**·$2C_6H_{14}$ each possess a disordered *tert*-butyl group. The disordered atoms of the ligands were addressed by assigning the groups in two positions. A summary of relevant crystallographic data for **$(Ar^*NH)_2CO$**, **$(Ar^*N)_2C$**, **Li[^{Ar}*ketguan]**, **K[^{Ar}*ketguan]**·$2C_6H_{14}$, and **Cs[^{Ar}*ketguan]**·Et_2O is presented in Table 2.

■ ASSOCIATED CONTENT

Supporting Information

X-ray crystallographic information (CIF), NMR, IR, and MS spectral data, ORTEP diagrams, and additional structures. This material is available free of charge via the Internet at http://pubs.acs.org.

■ AUTHOR INFORMATION

Corresponding Author

*E-mail: asfortier@utep.edu.

Notes

The authors declare no competing financial interest.

■ ACKNOWLEDGMENTS

This research was funded in large part by the University of Texas at El Paso with added support provided by the National Science Foundation (NSF) PREM program (Grant DMR-1205302) and the NSF American Competitiveness in Chemistry Fellowship (Grant CHE-1137284 to S.F). We thank Sudhakar Kalagara for assistance with the ATR FTIR measurements, Danisha M. Rivera-Nazario for assistance with MALDI-TOF-MS spectral analyses, and Dr. Sohan de Silva for assistance with the ESI-MS spectral analyses.

■ REFERENCES

(1) Piro, N. A.; Lichterman, M. F.; Harman, W. H.; Chang, C. J. *J. Am. Chem. Soc.* **2011**, *133*, 2108.

(2) MacBeth, C. E.; Golombek, A. P.; Young, V. G.; Yang, C.; Kuczera, K.; Hendrich, M. P.; Borovik, A. S. *Science* **2000**, *289*, 938.

(3) Yandulov, D. V.; Schrock, R. R. *Science* **2003**, *301*, 76.

(4) King, D. M.; Tuna, F.; McInnes, E. J. L.; McMaster, J.; Lewis, W.; Blake, A. J.; Liddle, S. T. *Nat. Chem.* **2013**, *5*, 482.

(5) Castro-Rodriguez, I.; Nakai, H.; Zakharov, L. N.; Rheingold, A. L.; Meyer, K. *Science* **2004**, *305*, 1757.

(6) Scepaniak, J. J.; Vogel, C. S.; Khusniyarov, M. M.; Heinemann, F. W.; Meyer, K.; Smith, J. M. *Science* **2011**, *331*, 1049.

(7) (a) Nguyen, T.; Sutton, A. D.; Brynda, M.; Fettinger, J. C.; Long, G. J.; Power, P. P. *Science* **2005**, *310*, 844. (b) Boynton, J. N.; Guo, J.-D.; Fettinger, J. C.; Melton, C. E.; Nagase, S.; Power, P. P. *J. Am. Chem. Soc.* **2013**, *135*, 10720. (c) Green, S. P.; Jones, C.; Stasch, A. *Science* **2007**, *318*, 1754. (d) Fischer, R. C.; Power, P. P. *Chem. Rev.* **2010**, *110*, 3877. (e) Chai, J.; Zhu, H.; Stückl, A. C.; Roesky, H. W.; Magull, J.; Bencini, A.; Caneschi, A.; Gatteschi, D. *J. Am. Chem. Soc.* **2005**, *127*, 9201. (f) Power, P. P. *Chem. Rev.* **2012**, *112*, 3482. (g) Carpenter, A. E.; Margulieux, G. W.; Millard, M. D.; Moore, C. E.; Weidemann, N.; Rheingold, A. L.; Figueroa, J. S. *Angew. Chem., Int. Ed.* **2012**, *51*, 9412. (h) Laskowski, C. A.; Miller, A. J. M.; Hillhouse, G. L.; Cundari, T. R. *J. Am. Chem. Soc.* **2010**, *133*, 771. (i) Hatanaka, T.; Miyake, R.; Ishida, Y.; Kawaguchi, H. *J. Organomet. Chem.* **2011**, *696*, 4046. (j) Li, T.; Schulz, S.; Roesky, P. W. *Chem. Soc. Rev.* **2012**, *41*, 3759. (k) Kays, D. L. *Dalton Trans.* **2011**, *40*, 769.

(8) Hicks, J.; Hoyer, C. E.; Moubaraki, B.; Manni, G. L.; Carter, E.; Murphy, D. M.; Murray, K. S.; Gagliardi, L.; Jones, C. *J. Am. Chem. Soc.* **2014**, *136*, 5283.
(9) Ni, C.; Power, P. P. *Chem. Commun.* **2009**, 5543.
(10) (a) Iwai, T.; Okochi, H.; Ito, H.; Sawamura, M. *Angew. Chem., Int. Ed.* **2013**, *52*, 4239. (b) Dierick, S.; Dewez, D. F.; Markó, I. E. *Organometallics* **2014**, *33*, 677.
(11) Jones, C. *Coord. Chem. Rev.* **2010**, *254*, 1273.
(12) Edelmann, F. T. *Adv. Organomet. Chem.* **2008**, *57*, 183.
(13) Berthon-Gelloz, G.; Siegler, M. A.; Spek, A. L.; Tinant, B.; Reek, J. N. H.; Markó, I. E. *Dalton Trans.* **2010**, *39*, 1444.
(14) Corbin, P. S.; Zimmerman, S. C.; Thiessen, P. A.; Hawryluk, N. A.; Murray, T. J. *J. Am. Chem. Soc.* **2001**, *123*, 10475.
(15) Coles, M. P. *Dalton Trans.* **2006**, 985.
(16) Uehara, K.; Mizuno, N. *J. Am. Chem. Soc.* **2011**, *133*, 1622.
(17) Stevens, C. L.; Singhal, G. H.; Ash, A. B. *J. Org. Chem.* **1967**, *32*, 2895.
(18) (a) Findlater, M.; Hill, N. J.; Cowley, A. H. *Dalton Trans.* **2008**, 4419. (b) Vincent, A. T.; Wheatley, P. J. *J. Chem. Soc., Perkin Trans. 2* **1972**, 1567. (c) Irngartinger, H.; Jager, H.-U. *Acta Crystallogr., Sect. B* **1978**, *34*, 3262.
(19) (a) A. R. Schmidt, J.; Arnold, J. *Chem. Commun.* **1999**, 2149. (b) Boere, R. T.; Klassen, V.; Wolmershauser, G. *J. Chem. Soc., Dalton Trans.* **1998**, 4147. (c) Boeré, R. T.; Klassen, V.; Wolmershäuser, G. *Can. J. Chem.* **2000**, *78*, 583.
(20) **Cs**[^{Ar*}**ketguan**] is isolated in moderate yields from a complicated product mixture containing unidentified orange by-products.
(21) Cordero, B.; Gomez, V.; Platero-Prats, A. E.; Reves, M.; Echeverria, J.; Cremades, E.; Barragan, F.; Alvarez, S. *Dalton Trans.* **2008**, 2832.
(22) Cole, M. L.; Davies, A. J.; Jones, C.; Junk, P. C. *J. Organomet. Chem.* **2004**, *689*, 3093.
(23) Boere, R. T.; Cole, M. L.; Junk, P. C. *New J. Chem.* **2005**, *29*, 128.
(24) Coles, M. P.; Hitchcock, P. B. *Aust. J. Chem.* **2013**, *66*, 1124.
(25) Lee, H. S.; Niemeyer, M. *Inorg. Chem.* **2006**, *45*, 6126.
(26) Wong, E. W. Y.; Dange, D.; Fohlmeister, L.; Hadlington, T. J.; Jones, C. *Aust. J. Chem.* **2013**, *66*, 1144.
(27) Jin, G.; Jones, C.; Junk, P. C.; Lippert, K.-A.; Rose, R. P.; Stasch, A. *New J. Chem.* **2009**, *33*, 64.
(28) Weinert, C. S.; Fanwick, P. E.; Rothwell, I. P. *Dalton Trans.* **2003**, 1795.
(29) Poater, A.; Cosenza, B.; Correa, A.; Giudice, S.; Ragone, F.; Scarano, V.; Cavallo, L. *Eur. J. Inorg. Chem.* **2009**, 1759.
(30) Willcocks, A. M.; Robinson, T. P.; Roche, C.; Pugh, T.; Richards, S. P.; Kingsley, A. J.; Lowe, J. P.; Johnson, A. L. *Inorg. Chem.* **2011**, *51*, 246.
(31) Glock, C.; Loh, C.; Görls, H.; Krieck, S.; Westerhausen, M. *Eur. J. Inorg. Chem.* **2013**, 3261.
(32) Coles, M. P.; Swenson, D. C.; Jordan, R. F.; Young, V. G. *Organometallics* **1998**, *17*, 4042.
(33) Clegg, W.; Snaith, R.; Shearer, H. M. M.; Wade, K.; Whitehead, G. *J. Chem. Soc., Dalton Trans.* **1983**, 1309.
(34) Odom, A. L.; Cummins, C. C. *Organometallics* **1996**, *15*, 898.
(35) *SMART Apex II*, version 2.1; Bruker AXS Inc.: Madison, WI, 2007.
(36) *SAINT Software User's Guide*, version 7.34a; Bruker AXS Inc.: Madison, WI, 2007.
(37) Blessing, R. *Acta Crystallogr., Sect. A* **1995**, *A51*.
(38) Sheldrick, G. M. *SHELXTL*, version 6.12; Bruker Analytical X-Ray Systems, Inc.: Madison, WI, 2008.
(39) Dolomanov, O. V.; Bourhis, L. J.; Gildea, R. J.; Howard, J. A. K.; Puschmann, H. *J. Appl. Crystallogr.* **2009**, *42*, 339.